Permittivity Change of NiZn Ferrite – $BaTiO_3$ Composites with Fe Content

Kazutomo Abe, Naoto Kitahara[1], Mikio Higuchi, and Junichi Takahashi
Division of Materials Chemistry, Graduate School of Engineering, Hokkaido University, Sapporo 060-8628, Japan
[1] Department of System Electronics and Information Technology, Faculty of Engineering, Tokyo Polytechnic University, Atsugi 243-0297, Japan

Key Words; Ceramic composite, $BaTiO_3$, NiZn ferrite, dielectric permittivity, Fe content, Ti-substitution

Abstract

Ceramic composites were fabricated from powder mixtures of $BaTiO_3$ and $Ni_{0.3}Zn_{0.7}Fe_xO_{4\pm\delta}$ with different Fe contents of x = 1.8, 1.9, 2.0, 2.1, and 2.2 to examine the effect of the Fe content on the dielectric permittivity (ε_r) of the composite samples. The ε_r values of the composites were greatly affected by the Fe content such that a small ε_r value of the Fe1.8 composite sample steeply increased with an increasing Fe content by about three orders of magnitude for the Fe2.1 and Fe2.2 samples. The strong Fe content dependence could be correlated with the incorporation of the Ti^{4+} ions into the octahedral sublattices in the ferrite structure. The Ti-substitution would preferentially contribute to charge compensation for the Fe-poor ferrites, whereas it should result in the creation of the Fe^{2+} ions on the octahedral sublattices of the Fe-rich ferrite phases. Therefore, the presence of the Fe^{2+} ions synergetically created by the Ti-substitution and Fe-rich composition would be responsible for the considerably increasing ε_r values for the Fe2.1 and Fe2.2 composite samples.

1. Introduction

Ceramic composites consisting of magnetic and dielectric oxides are one of the candidate materials for electromagnetic wave absorber (EWA) working in a wide frequency range. [1, 2)] The working performance of an EMA is strongly dependent on the impedance matching, $Z_0 = Z_1$, between air (impedance of Z_0) and the absorber material (Z_1). Each impedance can be related to its magnetic permeability and dielectric permittivity as follows;

$$Z_0 = (\mu_0 / \varepsilon_0)^{1/2} \quad \cdots (1)$$

$$Z_1 = (\mu_{r1} / \varepsilon_{r1})^{1/2} \tan h (\gamma_1 d_1) \quad \cdots (2)$$

where μ_0 and ε_0 are the permeability and permittivity of vacuum (air), while μ_{r1} and ε_{r1} indicate the relative permeability and permittivity of the absorber with a thickness d_1, respectively. A propagating constant of an electromagnetic wave with its propagating constant of an electromagnetic wave with its wavelength of λ in an absorber, γ_1, is expressed as [3, 4)]

$$\gamma_1 = j (2\pi / \lambda) (\mu_{r1} \varepsilon_{r1})^{1/2} \cdots (3)$$

Accordingly, μ_{r1} and ε_{r1} are required to be equal to establish the $Z_0 = Z_1$ condition, which results in the reduction in the reflection of the corresponding electromagnetic wave at the interface between the absorber and air.

The present authors have focused on the fabrication of ceramic composites in which various amounts of $BaTiO_3$ (BT) particles were dispersed in a matrix phase of $Ni_{0.3}Zn_{0.7}Fe_2O_4$ (NZ ferrite) to find out an optimum composition range indicating the achievement of the $\mu_{r1} = \varepsilon_{r1}$ condition. It has been found that the ceramic composites with small amounts of the BT mixing ratio of 3 – 5 vol% showed considerably high ε_r values [5)] than those calculated from the Lichtenecker's mixture formula .[6)] The enhanced ε_r has been explained by the creation of Fe^{2+} ions as a result of the Ti^{4+}-substitution for the Fe^{3+} ions on the octahedral B-sites in the spinel structure and the electron hopping between Fe^{2+} and Fe^{3+} in the ferrite matrix.[5)] This kind of a change in the Fe^{2+}/Fe^{3+} ratio in a ferrite phase can be also adjusted by controlling the Fe content in the ferrite composition. For the NiZn ferrite of $Ni_{0.3}Zn_{0.7}Fe_{2.0+\delta}O_{4.0-X}$, a slightly increasing δ could cause a conversion from the insulating nature of the stoichiometric sample of δ=0 to the conducting one based on n-type electron hopping by the presence of Fe^{2+} ions.[7)] In the present study, therefore, the NZ ferrite – BT composites were fabricated using NZ ferrite powders with different Fe contents and the effect of the Fe content on the ε_r values of the composite samples was examined to elucidate whether the similar effect induced by variable Fe contents could appear or not.

2. Experimental Procedure

Fixed amounts of commercially available raw materials of Fe_2O_3, NiO, and ZnO (Wako Pure Chemical Ind.) and distilled water were mixed in a plastic container using YSZ balls for 12 h to prepare a slurry with a given ferrite composition of $Ni_{0.3}Zn_{0.7}Fe_XO_{4\pm y}$ (X = 1.8, 1.9, 2.0, 2.1, and 2.2). A dried powder was calcined at 1000°C for 4 h in air and pulverized into a fine powder less than 1 μm. Each ferrite powder thus prepared was named as Fe1.8, Fe1.9, Fe2.0, Fe2.1, and Fe2.2 ferrite hereafter. In the next process, a fixed amount of a commercially available $BaTiO_3$ powder (Sakai Chemical Industry Co., d_{av} = 0.5 μm) was added to a fine NZ ferrite powder, which was followed by mixing in a wet state to obtain various composite powders containing 3, 8, and 15 vol% BT (They are called 3BT, 8BT, and 15BT, respectively, in this study.). Green compacts formed by a uniaxial pressing at 50 MPa were sintered at 1250°C for 4 h in air and furnace-cooled. The sintered composite samples are referred to as, in this study, Fe1.8, Fe1.9, Fe2.0, Fe2.1, and Fe2.2 composites based on the corresponding Fe content in each ferrite. Sintered samples were characterized by density measurement (Archimedes method), solid phase identification with XRD (Rigaku Rint 2200), microstructure observation with SEM (JEOL JSM-6300F), and element analysis with EDS (JEOL JSM-6390LVS). For the evaluation of electrical properties, sintered composites were coated with Ag electrodes. Dielectric permittivity and DC resistivity of the composite samples were measured using an impedance analyzer (Agilent 4285A) and an electrometer (ADCMT 8340A) equipped with a DC supply (Agilent E3649A), respectively.

3. Results and Discussion

3.1 Phase and microstructure changes with Fe content

Figure 1 shows ε_r changes as a function of BT mixing ratio for the Fe1.8, Fe1.9, Fe2.0, and Fe2.2 composites. Depending on the Fe content in the NZ ferrite, substantial variations were recognized for the ε_r change with BT ratio. For composites containing the NZ ferrites with less Fe contents than the stoichiometric value of X = 2.0, i.e., Fe1.8 and Fe1.9 composites, no or slight and gradual increase in ε_r was observed with an increasing BT ratio. On the contrary, a very steep increase in ε_r by two or three orders of magnitude took place for the Fe2.0 and Fe2.2 composites.

In order to elucidate some causes leading to the substantially different behaviors in the ε_r change with BT ratio, phase changes during sintering were examined with the corresponding

microstructure evolution. XRD patterns of the 8BT composites are demonstrated as a function of Fe content in Fig.2. From the serial change in the XRD profiles with the Fe content, major solid phases newly formed during sintering could be classified into two groups; one detected in the Fe-poor (Fe1.8 and Fe1.9) and Fe2.0 composites, and the other in the Fe-rich (Fe2.1 and Fe2.2) composites. Then, taking the Fe1.8 and Fe2.2 composites as a representative in each group, comparative examinations were made by solid phase identification and microstructure observation combined with element analysis. Relative phase changes with BT ratio and typical BSEM images can be seen in Fig.3 and Fig.4, respectively. For the Fe1.8 samples, the formation of two kinds of a solid phase was detected and they were identified with $BaFe_2O_4$ and hexagonal-type $BaTiO_3$ (h-BT) phases. Detailed composition analysis showed that the composition of the $BaFe_2O_4$ phase formed in both the 8BT and 15BT composites was almost the same, i.e., $Ba(Fe_{1.9}Zn_{0.1})O_4$. On the contrary, the formation of the h-BT phase could be explained by the fact that the hexagonal structure of the $BaTiO_3$ phase is stabilized by the Fe-substitution for the Ti^{4+}-sites.[8, 9] Furthermore, the composition of the h-BT phases was found to show a strong dependence on the BT ratio. The Ti:Fe ratio in each h-BT phase changed from 8:92 to 64:36 for the 8BT to 15BT composites, respectively. Microstructure of the 8BT composite samples with Fe1.8 ferrite (Fig.4 (A-1)) was characterized by the presence of wedge-shaped regions. The appearance of the same solid phases ($BaFe_2O_4$ss and h-BTss) and very similar microstructure was observed for the stoichiometric Fe2.0 composite sample. As has been described in the previous study on the Fe2.0 composites, [5] a liquid phase formed in the psudobinary eutectic system of $BaFe_2O_4$ss and h-BTss should be responsible for the appearance of the wedge-shaped regions where h-BTss grains were deposited from the liquid while $BaFe_2O_4$ss grains consolidated during cooling process. In addition, the amount and composition of a liquid phase formed during sintering would be substantially different from composite to composite depending on the Fe content in the ferrite phase as well as BT ratio. Thus, this could explain the microstructure difference between Fe1.8 and Fe2.0 composites (Fig.4) and changes related to the h-BT phases in the Fe1.8 composites.

In the case of Fe-rich composites, a new compound appeared in both the Fe2.1 and Fe2.2 samples (Fig.2 & Fig.3), which showed considerably different microstructures from those of the Fe1.8 and Fe2.0 composites (Fig.4). Rectangular grains in Fig.4 (C-1) and (C-2) could be identified with the $Ba_2Fe_6O_{11}$ solid solutions containing Ni^{2+}, Zn^{2+}, and Ti^{4+} ions for the Fe^{3+}-sites. Approximate compositions were estimated to be $Ba_2(Fe_{4.35}Ni_{0.25}Zn_{0.6}Ti_{0.8})O_{11}$ and $Ba_2(Fe_{4.25}Ni_{0.25}Zn_{0.6}Ti_{0.9})O_{11}$ for 8BT and 15BT composites, respectively, irrespective of the Fe

content in the Fe-rich NZ ferrites. It was reported that the $Ba_2Fe_6O_{11}$ phase was a metastable phase in the psudobinary system of $BaFe_2O_4$ – $BaFe_{12}O_{19}$ and underwent a peritectoid decomposition to form both end members in the system at 1150°C. [10, 11] In this study, the $Ba_2Fe_6O_{11}$ss phase could be detected in the composite samples fabricated by sintering at 1250°C. It would be stabilized by the extensive substitution of various cations for the Fe^{3+}-sites. An additional and appreciable change observed for the Fe-rich composites was the appearance of the tetragonal BT phase at 15BT composite samples. As clearly seen in Fig.4 (C-2), a substantial amount of t-BT particles added to a starting mixture remained as fine particles as they would be dispersed in an original composite powder (Similar fine t-BT particles are present in the 15BT composite with the Fe2.0 ferrite in Fig.4 (B-2).). Thus, corresponding to the Fe content in the NZ ferrite and BT mixing ratio, appreciable changes in the solid phase formed and resulting microstructure could be recognized for the present NZ ferrite – BT composite samples.

3.2 Ti-substitution and related changes

In a previous study on the similar composites containing the Fe2.0 ferrite, a steep increase in ε_r observed for the composite samples with 3 ~ 5 vol% BT could be closely correlated with the Ti^{4+}-substitution for the Fe^{3+}-sites in the ferrite structure. [5] Based on the result of the previous study and no appreciable correlation between the phase formation behavior and ε_r changes in the present composite samples, the present authors have examined the Ti-substitution behavior for composite samples with different Fe contents and the resulting effect of the Ti-substitution on the DC resistivity of the composites fabricated in this study. Figure 5 shows changes in the Ti concentration incorporated into each ferrite phase with BT ratio for composites having a fixed amount of Fe content. It could be seen that the Ti concentration primarily increased with an increasing BT ratio for all the composites. It should be also noticed that the lower the Fe content in the NZ ferrite became, the larger the amount of Ti^{4+} ions incorporated into the corresponding ferrite phase could be. Since it became clear that the Ti-substitution necessarily occurred in the NZ ferrite – BT composite samples sintered at 1250°C, the DC resistivity changes with the Ti concentration incorporated were estimated for those composite samples. Linear characteristic of the V – I relationship was confirmed for all the composite samples. As can be seen in Fig.6, a relationship between DC resistivity and Ti concentration substantially changed in a different manner depending on the Fe content in each ferrite phase. For composite samples composed of the stoichiometric Fe (Fe2.0) and Fe-rich (Fe2.1 and Fe2.2) ferrite phases, increasing Ti concentration resulted in the considerable

decrease in the DC resistivity. Especially, it should be noticed that a very small amount of Ti-substitution caused a very steep lowering in the resistivity by two or three orders of magnitude for the Fe2.1 and Fe2.2 composites. On the other hand, the Fe-poor composite samples showed a restricted lowering in the resistivity (Fe1.9) or inversely increasing resistivity at higher amounts of Ti-substitution (Fe1.8). The different behaviors of the DC resistivity changes could be explained by considering different roles of the Ti-substitution and correlated creation of Fe^{2+} ions in the ferrite phase.

According to the fundamental effect of the Fe content on the resistivity of the NZ ferrite, the Fe-rich compositions imply the presence of some Fe^{2+} ions and the occurrence of n-type electron hopping, whereas the charge balance for the Fe-poor compositions may in part be maintained by the formation of oxygen vacancies or by the exclusion of some parts of the Ni and Zn components from the ferrite.[7)] Relatively high values of the DC resistivity of the Fe-rich ferrite samples without BT mixing might be due to partial oxidation of the Fe^{2+} ions during cooling from the sintering temperature. For the stoichiometric Fe and Fe-rich ferrites, the incorporation of the Ti^{4+} ions into the octahedral Fe^{3+}-sites definitely create the corresponding amount of the Fe^{3+} ions on the same sublattices. Therefore, a considerable and steep decrease in the resistivity observed for the Fe2.1 and Fe2.2 composite samples having a very small amount of the Ti-substitution could be essentially attributed to the creation of the Fe^{2+} ions. In this case, the creation of the Fe^{2+} ions was enhanced by synergetic effect of excess Fe content and the Ti-substitution. It was also found that the oxidation of the Fe^{2+} ions during cooling process would be effectively inhibited when the Fe^{2+} ions were produced by chemical modification such as Ti-substitution made in this study. For the Fe-poor ferrites, on the contrary, the Ti-substitution could preferentially contribute to charge compensation for the cation deficiency of the ferrite, which was originated from the Fe-poor composition, rather than to the creation of the Fe^{2+} ions on the octahedral sublattices. Thus, different resistivity values between the Fe1.9 and Fe1.8 composite samples at higher Ti concentrations could be closely correlated with what would be a major contribution induced by the Ti-substitution. It was used for the charge compensation only for the Fe1.8 composites, whereas it additionally played a role to create a very small amount of the Fe^{2+} ions as well as to make the charge compensation for the Fe1.9 composite samples.

In summary, the dependences of the ε_r of the representative composite samples containing 8 and 15 vol% BT on the Fe content are given in Fig.7 with the corresponding changes in the resistivity. Each composite with a fixed BT ratio reveals a strong Fe content dependence for both ε_r and resistivity changes. The resistivity changes with the Fe content could

be explained by different contributions of the Ti-substitution for ferrite phases with different Fe contents. Therefore, the presence of the Fe^{2+} ions created synergetically by the Fe-rich composition and Ti-substitution definitely led to considerable increases in the apparent ε_r values of the Fe2.1 and Fe2.2 composite samples. From this study, enhanced ε_r values were found to come from the electrical conductive nature of the modified ferrite phase. So an attempt such as surface coating of BT particles will be made to control the reactions occurring during sintering and give the exact dielectric contribution inherent to the ferroelectric BT phase to the present composite system in the following study.

4. Conclusion

NiZn ferrite – $BaTiO_3$ ceramic composites were fabricated using $Ni_{0.3}Zn_{0.7}Fe_XO_{4\pm\delta}$ powders in which the Fe content was controlled to be X= 1.8 and 1.9 (Fe-poor) and X = 2.1 and 2.2 (Fe-rich) in addition to the stoichiometric X = 2.0 to elucidate the effect of the Fe content on the dielectric permittivity (ε_r) of the resulting ceramic composites. From XRD analysis and microstructure observation, secondary phases produced during sintering were found to be different depending on the Fe content. The $BaFe_2O_4$ss and hexagonal-type $BaTiO_3$ss phases were detected in the Fe-poor composites, whereas the $Ba_2Fe_6O_{11}$ss phase appeared in the Fe-rich ones. However, the formation of these new solid phases could not be directly associated with the ε_r changes showing a strong Fe content dependence. Element analysis with EDS and DC resistivity measurement revealed that the ε_r changes could be closely correlated with the resistivity changes and the strong Fe content dependence of the resistivity changes would result from different contributions of the Ti-substitution for ferrite phases. Taking account of the fundamental effect of the Fe content on the resistivity of the NZ ferrite and the additional effect of the Ti-substitution, different behaviors of the resistivity changes between the Fe-rich and Fe-poor composites could be explained. A considerable and steep decrease in the resistivity observed for the Fe-rich samples at a very small amount of the Ti-substitution was essentially due to enhanced creation of the Fe^{2+} ions on the octahedral sublattices, which were synergetically produced by the Fe-rich composition and Ti-substitution. For the Fe-poor composites, on the contrary, the Ti-substitution would preferentially play a role as charge compensation for the cation deficiency originated from the Fe-poor composition, leading to much higher resistivity values.

Acknowledgement

This study was partly supported by the Global COE Program (Project No. B01: Catalysis as the Basis for Innovation in Materials Science) from the Ministry of Education, Culture, Sports, Science and technology, Japan.

References

1) Xiwei Qi, Ji Zhou1, Zhenxing Yue, Zhilun Gui, Longtu Li,:J. Magn. Magn. Mater., **269** (2004) 352.

2) N. Kitahara, T. Mizumoto:IEICE Trans C, **J86-C No4** (2003) 450.

3) M.P.Horvath:J. Magn. Magn. Mater., **215-216** (2000) 171.

4) Y.Naito, K.Suetake:IEEE Transactions, **MIT-10 No.1** (1971) 65.

5) K. Abe N.Kitahara, M.Higuchi and J.Takahashi: submitted to J. Ceram. Soc. Japan.

6) Kuo-Chung Cheng, Chien-Ming Lin, Sea-Fue Wang, Shun-Tian Lin, Chang-Fa Yang :Mater.Lett., **61-3** (2007) 757.

7) A.J.Moulson and J.M.Herbert: *Electroceramics, 2nd ED* (John Wiley & Sons Ltd, Chichester, 2003) p.496-501

8) N. Masó, H. Beltrán, E. Cordoncillo, P. Escribano and A. R. West : J. Mater. Chem., **16** (2006) 1626.

9) Ian E. Grey, Christina Li, Lachlan M. D. Cranswick, Robert S. Roth, and Terrell A. Vanderah: J. Solid State Chem., **135** (1998) 312.

10) G. Sloccari: J. Amer. Ceram. Soc., **56** (1973) 489-90.

11) T. A. Vanderah, J. M. Loezos, and R. S. Roth: J. Solid State Chem., **121** (1996) 38.

Figure captions

Fig.1 ε_r changes with BT ratio for composites with different Fe contents.

Fig.2 XRD patterns of the 8BT composites with different Fe contents.

(●NiZn ferrite, ▲t-$BaTiO_3$, ○$BaFe_2O_4$ss, ▽h-$BaTiO_3$ss, □$Ba_2Fe_6O_{11}$ss)

Fig.3 Fractional solid phase content in (A) Fe1.8 and (B) Fe2.2 composites.

($Ba_2Fe_6O_{11}$ss, $BaFe_2O_4$ss, t-$BaTiO_3$,

h-$BaTiO_3$ss, NiZn ferrite)

Fig.4 BSEM images of (A) Fe1.8, (B) Fe2.0, and (C) Fe2.2 composites with BT ratio of (1) 8 vol% and (2) 15 vol%.

Fig.5 Ti concentration changes with BT ratio for composites with different Fe contents.

Fig.6 DC resistivity vs. Ti concentration for composites with different Fe contents.

Fig.7 Fe content dependences of ε_r and DC resistivity for 8BT and 15BT composites.

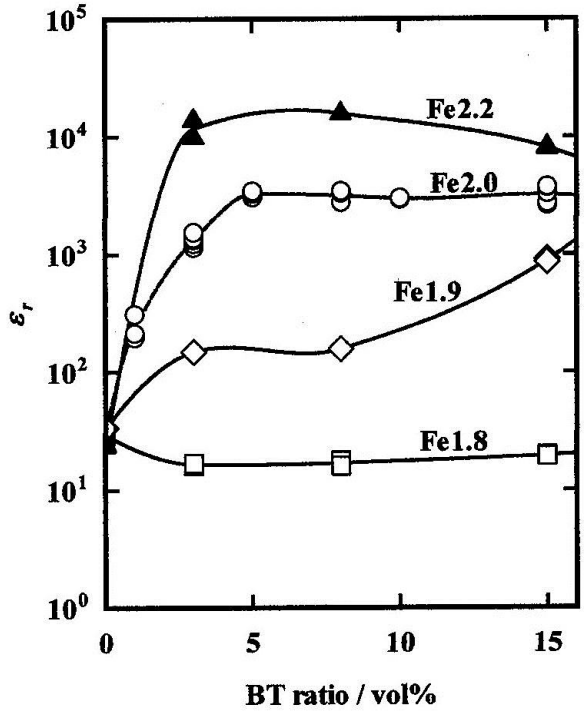

Fig.1 ε_r changes with BT ratio for composites with different Fe contents.

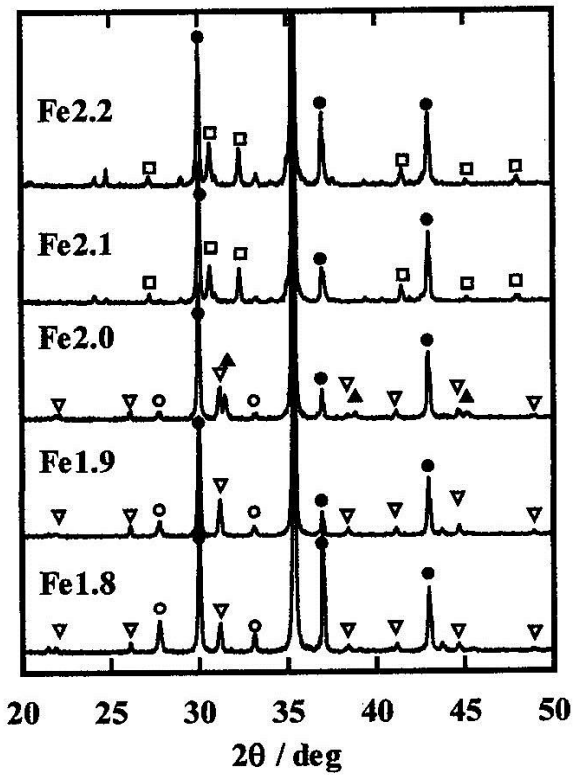

Fig.2 XRD patterns of the 8BT composites with different Fe contents.
(●NiZn ferrite, ▲t-$BaTiO_3$, ○$BaFe_2O_4$ss, ▽h-$BaTiO_3$ss, □$Ba_2Fe_6O_{11}$ss)

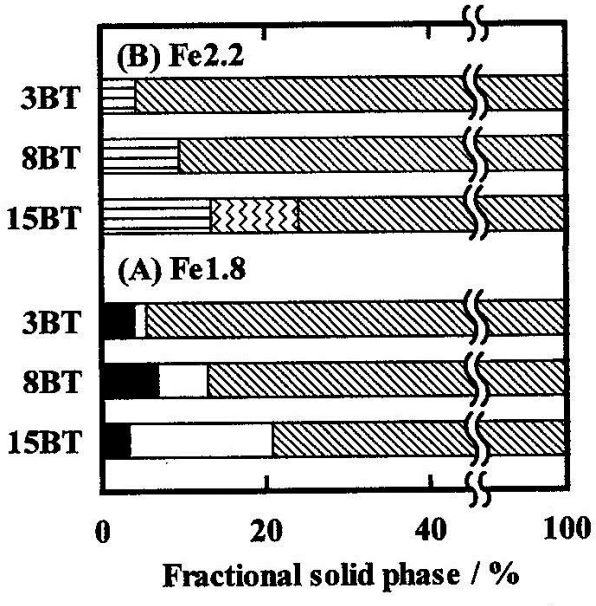

Fig.3 Fractional solid phase content in (A) Fe1.8 and (B) Fe2.2 composites.
($Ba_2Fe_6O_{11}$ss, $BaFe_2O_4$ss, t-$BaTiO_3$,
h-$BaTiO_3$ss, NiZn ferrite)

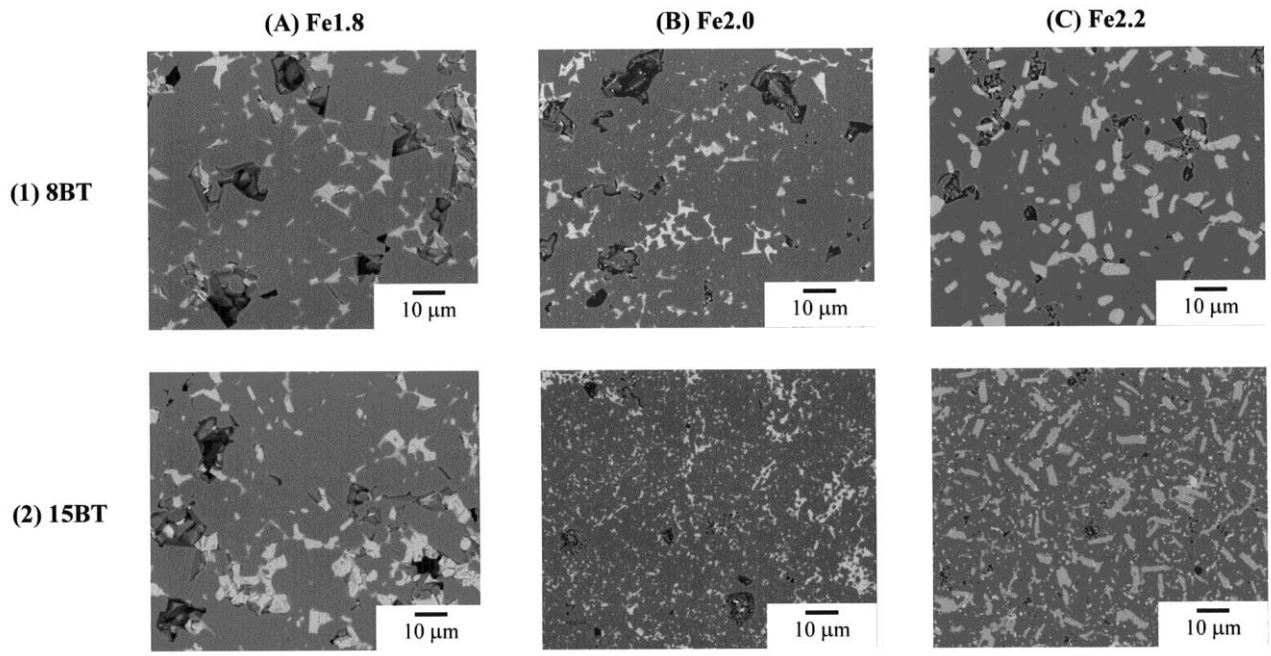

Fig.4 BSEM images of (A) Fe1.8, (B) Fe2.0, and (C) Fe2.2 composites with BT ratio of (1) 8 vol% and (2) 15 vol%.

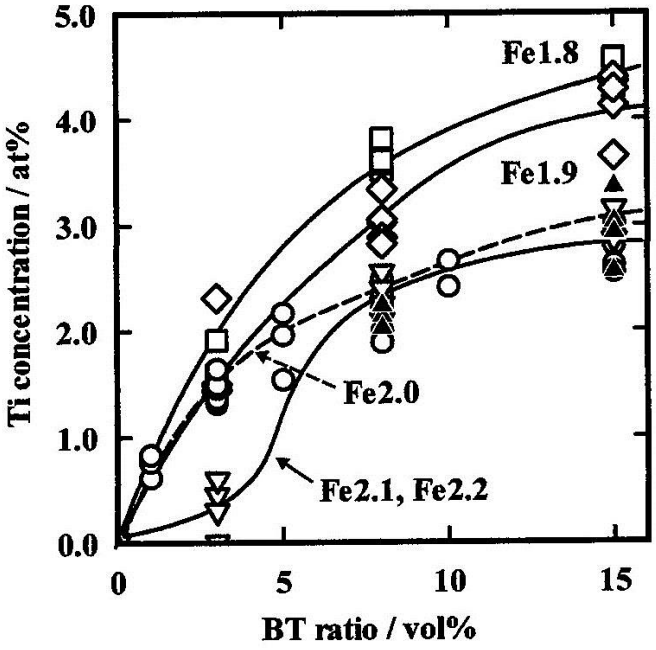

Fig.5 Ti concentration changes with BT ratio for composites with different Fe contents.

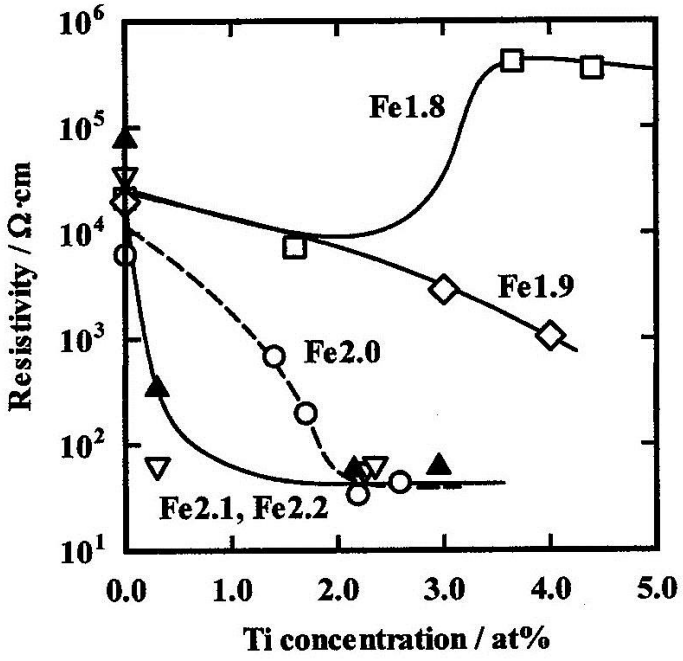

Fig.6 DC resistivity vs. Ti concentration for composites with different Fe contents.

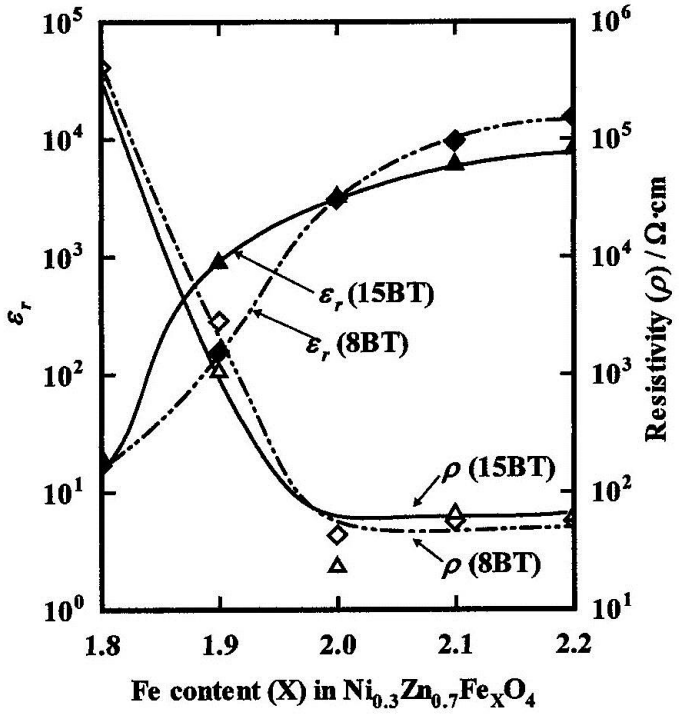

Fig.7 Fe content dependences of ε_r and DC resistivity for 8BT and 15BT composites.